

红杂色沉积建造中铀矿化的特殊岩石矿物特征 ——以库车坳陷新近系吉迪克组铀矿点为例

郭 强¹, 肖 菁¹, 刘 念¹, 王强强², 许 强¹, 武 勇¹, 严张磊¹, 刘梦魁¹,
丁 桐¹

(1. 核工业北京地质研究院, 北京 100029; 2. 核工业二一六大队, 新疆 乌鲁木齐 830011)

摘要: 近年来, 我国北方砂岩型铀矿勘查在中新生代红杂色沉积建造中不断取得找矿突破, 但关于红层中的铀成矿作用机制存在较大争议, 成为当前研究的热点。库车坳陷新近纪红层中发育大量铀矿化露头信息, 开展相关研究有助于分析红杂色层中铀富集机理。通过系统的沉积学、岩石学及矿物学研究对吉迪克组红杂色层铀矿化点进行解剖, 发现了较为特殊的铀矿化类型: 矿化层产于干旱背景下湖相沉积环境, 呈薄层透镜状产于大套红色泥岩中, 矿化岩性为灰绿色泥灰岩并发育大量红化硅质团块, 矿化具有层控特征并与硅质团块密切相关, 硅质团块具有红化微晶石英、萤石、铀石、方解石以及少量自然砷、黄铜矿和重晶石共生矿物组合, 与华南花岗岩型硅质脉铀矿化极为相似, 显示出深部热液成因特征; 综合判断该矿化层具有沉积和热液双重作用, 是特殊的热水沉积型铀矿化。这类铀矿化的发现为深部热液携带铀进入沉积盆地发生铀成矿作用带来直接有力证据, 丰富了陆相盆地沉积型铀成矿理论。

关键词: 库车坳陷; 新近纪; 吉迪克组; 红杂色层; 硅质团块; 热液铀矿化

中图分类号: P619. 14

文献标识码: A

文章编号: 1000-6524(2024)05-1268-13

Special rock and mineral characteristics of uranium mineralization in red variegated sedimentary formations: Taking the uranium occurrence of Neogene Jidike Formation in Kuqa Depression as an example

GUO Qiang¹, XIAO Jing¹, LIU Nian¹, WANG Qiang-qiang², XU Qiang¹, WU Yong¹, YAN Zhang-lei¹,
LIU Meng-kui¹ and DING Tong¹

(1. Beijing Research Institute of Uranium Geology, Beijing 100029, China; 2. Geologic Party No. 216, CNNC, Urumqi 830011, China)

Abstract: In recent years, the exploration of sandstone-type uranium deposits in the northern part of China has made breakthroughs in the Mesozoic and Cenozoic red-colored sedimentary formations. However, there is a great controversy about the mechanism of uranium mineralization in red beds, which has become a hot topic of current research. A large amount of uranium mineralization outcrop information is developed in the Neogene red layer in the Kuqa Depression. Carrying out relevant research is very helpful in analyzing the uranium enrichment mechanism in the red variegated layer. Through systematic sedimentology, petrology and mineralogy, the uranium mineralization spots in the red variegated layer of the Jidike Formation were dissected, and a relatively special type of uranium mineralization was discovered: the mineralized layer was located in a lacustrine sedimentary environment under an

收稿日期: 2023-12-26; 接受日期: 2024-06-01; 编辑: 尹淑萍; 英文审校: 王 丹

基金项目: 中核集团“青年英才”科研项目(QNYC2202)

作者简介: 郭 强(1982-), 男, 正高级工程师, 从事沉积学、砂岩型铀矿研究, E-mail: guoqiang9818@126.com。

arid background. It is produced in a large set of red mudstone in the shape of a thin layer of lens. The mineralization lithology is gray-green marl and develops a large number of reddened siliceous masses. The mineralization has layer-controlled characteristics and is closely related to the siliceous masses. The siliceous mass has a combination of reddish microcrystalline quartz, fluorite, uranite, calcite and a small amount of natural arsenic, chalcopyrite and barite intergrowth minerals. The siliceous mass is very similar to the granite-type siliceous vein uranium mineralization in South China, showing the characteristics of deep hydrothermal origin. It is comprehensively judged that this mineralized layer has dual effects of sedimentation and hydrothermal fluid, and is a special hot water deposition type uranium mineralization. This type of uranium mineralization discovery provides direct and strong evidence that deep hydrothermal fluids could carry uranium into sedimentary basins to undergo uranium mineralization, and improve the theory of sedimentary uranium mineralization in continental basins.

Key words: Kuqa Depression; Neogene; Jidike Formation; red variegated layer; siliceous mass; hydrothermal uranium mineralization

Fund support: Young Elite Project of China National Nuclear Corporation (QNYC2202)

库车坳陷中、新生界蕴藏着数十个砂岩型铀矿(化)点及异常点,矿化层位自北向南具有由老变新的特点,中生界铀矿化主要分布于北部近天山的构造带,库车坳陷南部秋里塔格构造带为重要的新生界铀成矿带(刘刚等, 2010; 庄红红等, 2015; 鲁克改等, 2019; 许强等, 2019; 吴立群等, 2022; 李盛富, 2023; 师志龙, 2023; 王国荣等, 2023),尤其是秋里塔格构造带西段发育大量赋存于古近系、新近系的铀矿化点,这些铀矿化主要赋存于大套红杂色层中的灰绿色砂岩和泥岩中,前人将这些铀矿化统归为砂岩型铀矿,认为矿化成因类型以同生沉积、后生淋滤和后生氧化为主(王新华等, 2012)。本次调查研究新近系铀矿化点时,发现秋里塔格西段吉迪克组某段铀矿化与传统砂岩型铀矿化有较大差别。通过系统的岩石学和矿物学研究,认为该处铀矿化具有明显的同沉积热液作用特征,强调了沉积盆地深部来源铀的重要性,为北方中新生代沉积盆地砂岩型热液铀成矿作用观点提供了直接有力的证据。

1 地质背景

库车坳陷位于塔里木盆地北缘,是南天山造山带与塔北隆起之间的中、新生代前陆盆地,自南天山向前陆方向依次划分为北部单斜带、直线褶皱带、拜城凹陷、秋里塔格复背斜、乌什凹陷、南部平缓背斜带和阳霞凹陷7个二级构造单元(图1a)(汤良杰等, 2008)。秋里塔格复背斜位于库车前陆盆地前缘冲断带,总体走向为NEE向,展布形态呈现略向南凸出的不对称弧形,西邻乌什凹陷,东接阳霞凹

陷,东西延伸320 km。该构造带形成于喜山晚期强烈构造挤压应力环境之中,发生褶皱变形和冲断作用,褶皱抬升和冲断抬升使得新生界出露地表遭受风化剥蚀(李世琴等, 2013; 王珂等, 2022; 王元元等, 2023),产于古近系、新近系的铀矿(化)点及异常点也随之出露地表,为矿点解剖研究提供了便利。

秋里塔格构造带由一系列断背斜、半背斜及断鼻组成,具有北缓南陡的特征,地表核部出露最老地层为古近系苏维依组,向两翼依次出露新近系吉迪克组、新近系康村组和新近系库车组,以库车组分布最为广泛(图1b)。中新统吉迪克组俗称“条带岩组”,在秋里塔格构造带核部主要呈窄条状分布,由褐红色泥岩夹多层的灰绿色砂岩、泥岩条带以及厚膏盐岩沉积组成(张师本等, 2003),整体表现为干旱环境扇三角洲-盐湖沉积。本次研究的铀矿点位于秋里塔格构造带西端博孜墩南一带(图1b),新近系吉迪克组在此大面积出露,铀矿化产于吉迪克组中下部。

2 铀矿化产出特征

2.1 铀矿化层产出沉积环境

库车坳陷吉迪克组沉积时期,气候干旱、炎热,蒸发岩沉积极为发育,该组自下而上由砂砾岩段、膏泥岩段、砂泥岩段、膏盐岩段和泥岩段5个沉积岩段组成(王利刚, 2004; 时文革等, 2015),整体以扇三角洲、正常三角洲和湖泊沉积相为主(谭秀成等, 2006; 张萱等, 2023)。吉迪克组沉积相东西差异、南北分异明显(图2),中-西部发育扇三角洲-湖相

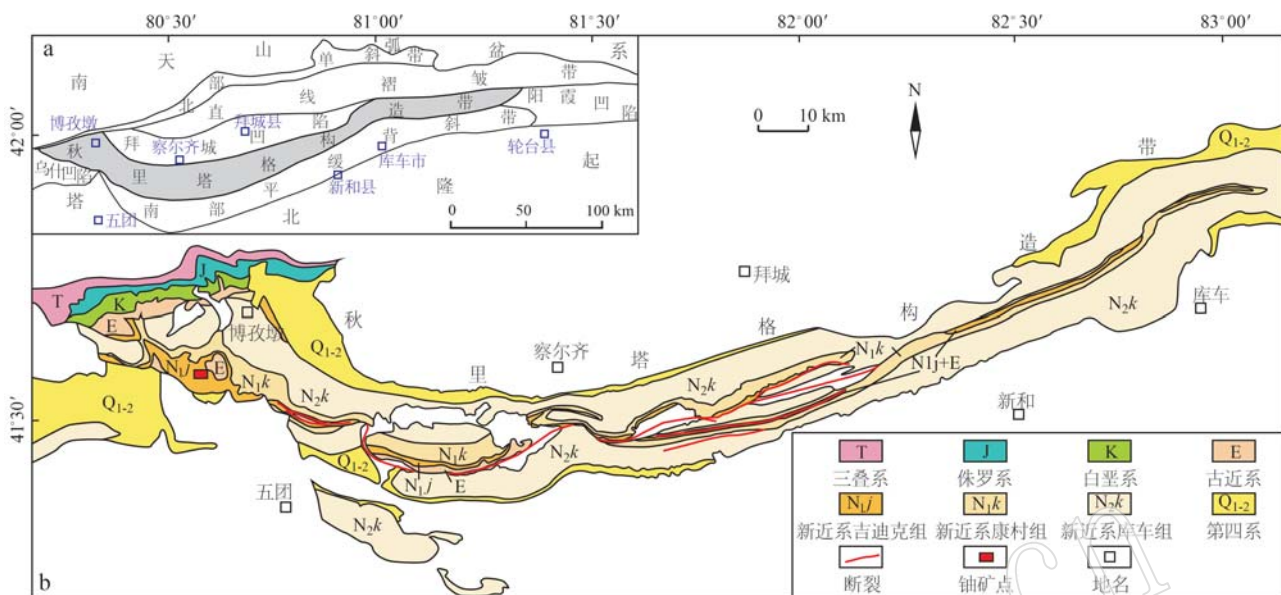


图1 库车坳陷秋里塔格构造带地质简图(a, 据汤良杰等, 2008 修改)及研究铀矿点位置(b, 阿种明等, 2007 修改)

Fig. 1 Simplified geological map of the Qiulitage structural belt in the Kuqa Depression (a, from Tang Liangjie et al., 2008) and the location of the studied uranium deposits (b, modified from A Zhongming et al., 2007)

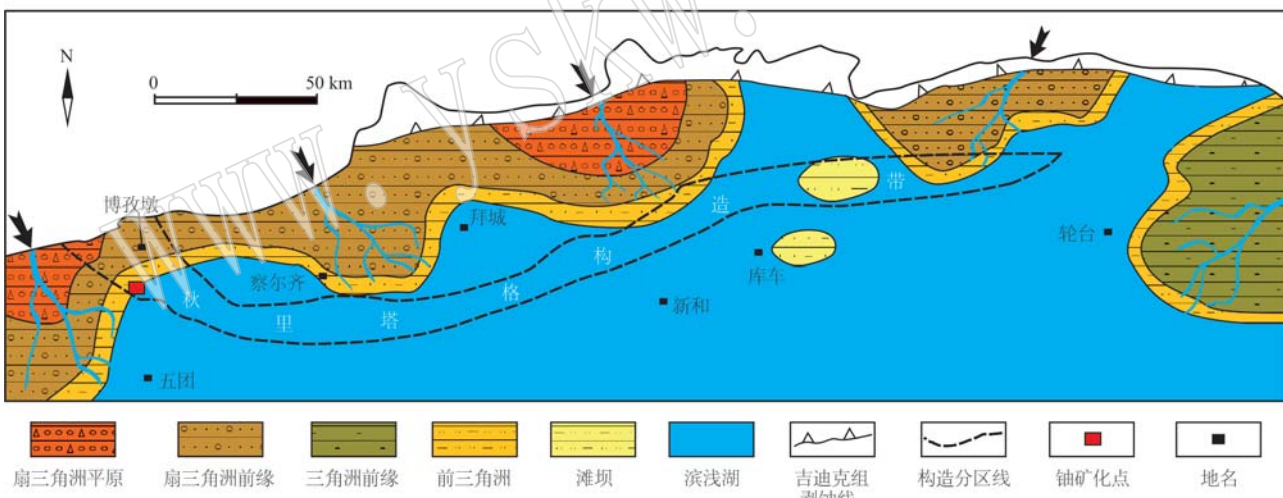


图2 库车坳陷吉迪克组沉积相平面展布图(据谭秀成等, 2006; 张萱等, 2023 修改)

Fig. 2 Plane layout of sedimentary facies of the Jidike Formation in the Kuqa Depression (modified from Tan Xiucheng et al., 2006; Zhang Xuan et al., 2023)

沉积, 东部发育正常三角洲-湖相沉积, 其中所含膏盐岩自西向东逐渐变厚; 自北向南依次发育扇三角洲平原、扇三角洲前缘、前三角洲、滩坝和滨浅湖, 以秋里塔格构造带为界, 北部主要分布扇三角洲前缘-前三角洲-滩坝-滨浅湖沉积, 南部主要分布滨浅湖沉积, 其中滨浅湖沉积岩相也具有明显的南北分异特征, 北部以膏泥岩相为主, 秋里塔格构造带以南膏岩沉积逐渐较少, 过渡为泥岩相。研究区位于前三

角洲和滨浅湖过渡区域, 沉积岩性以厚层膏泥岩和席状砂为主要特征, 铀矿化就产于这种干旱气候条件下的三角洲-湖泊沉积体系中。

2.2 铀矿化层产出沉积序列

研究区吉迪克组沉积剖面自下而上由滨浅湖-前扇三角洲-扇三角洲前缘构成不完整反旋回相序(图3), 垂向上不发育扇三角洲平原亚相。滨浅湖沉积剖面上表现为厚层膏泥岩(图3a)与紫褐色、棕

红色泥岩不等厚互层出现,表现出该时期湖泊为氧化宽浅型(李维锋等,1996),湖水进退频繁,在干旱古气候背景下滨浅湖沉积红色泥岩和频繁出现的石膏层,当季节性洪水补给陆源碎屑,蒸发岩相则会夹杂薄层碎屑沉积(宋金鹏等,2021)(图3b)。前扇三角洲沉积剖面上主要表现为大套块状红色泥岩,

偶夹薄层或透镜状砂岩,铀矿化层产于此沉积段。扇三角洲前缘沉积剖面上可明显识别出席状砂和河口坝微相,席状砂微相沉积表现为薄层状砂岩与泥岩互层(图3c),见明显的透镜状、脉状层理(图3d);河口坝微相沉积表现为泥-粉砂-中砂反韵律(图3e),砂岩中见明显的波痕层面构造(图3f)。

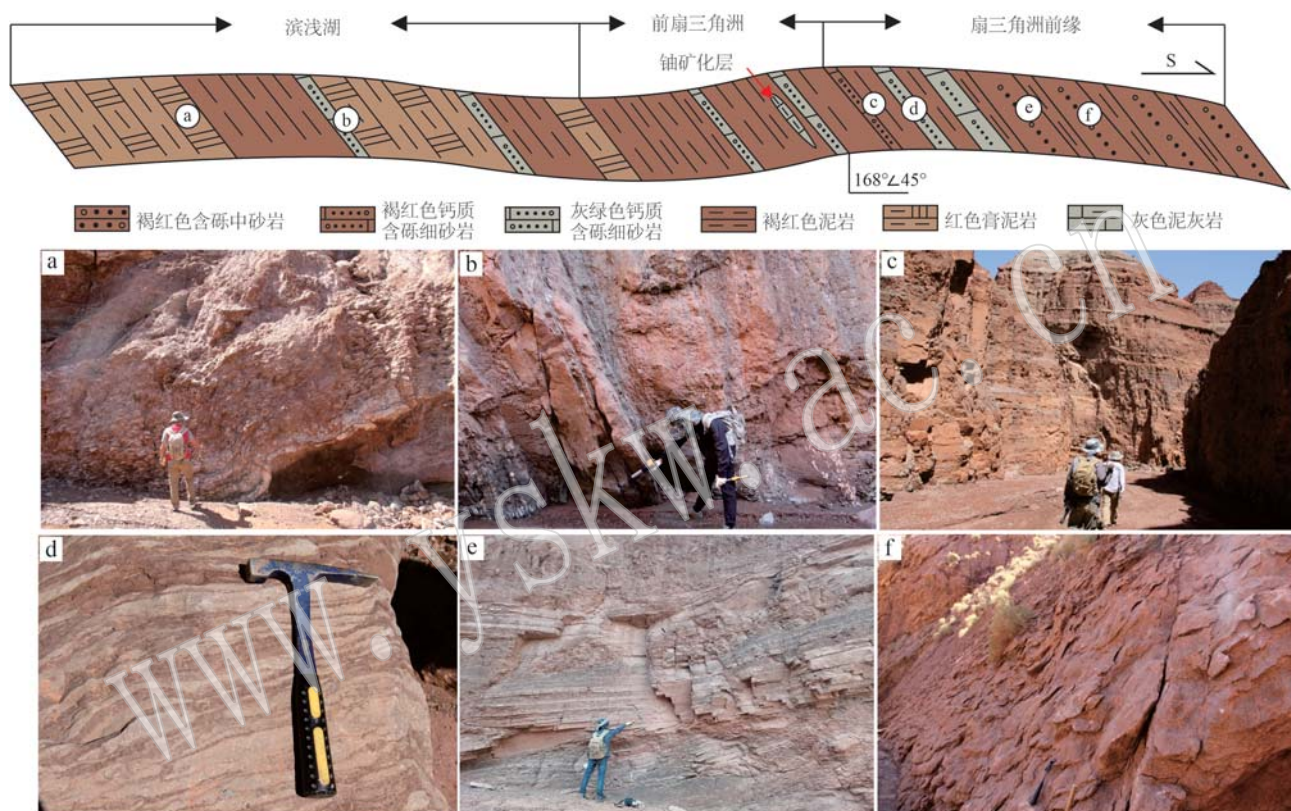


图3 吉迪克组含矿段沉积旋回示意剖面图及典型照片

Fig. 3 Schematic cross-section and typical photos of sedimentary cycles in the ore-bearing section of the Jidike Formation

a—厚层状膏岩与红色泥岩不等厚互层; b—大套膏泥岩夹透镜状砂岩; c—大套褐红色泥岩夹席状灰色、灰绿色、褐红色砂岩;

d—透镜状、脉状层理; e—中厚层状砂岩与泥岩构成下细上粗反旋回特征; f—红色砂岩层面发育的波痕

a—the thick bedded gypsum and red mudstone are interbedded with unequal thicknesses; b—a large suite of gypsiferous mudstone interbedded with lenticular sandstone; c—a large set of brownish-red mudstone interbedded with tabular gray, gray-green, and brownish-red sandstone; d—lenticular and vein-like bedding; e—medium to thick-bedded sandstone and mudstone form a fining-upward coarsening-upward cyclothem characteristic; f—the wavy bedding phenomenon developed on the surfaces of red sandstone layers

2.3 铀矿化层沉积岩性特征

铀矿化层产于大套红色泥岩的浅色层,前人共发现7个含矿层和4种含矿岩性(蔡兰朋等,1985;王新华等,2012),含矿层呈层状、似层状及凸镜状,矿化层沿NEE走向连续而均匀分布,但厚度较小(0.55~0.90 m),品位0.034%~0.148%;含矿岩性为灰绿色粉砂质泥岩、灰绿色结核状泥灰岩、灰红色

-灰绿色砂岩和杂色含铁硅质岩。本文重点解剖的为灰绿色硅质团块泥灰岩这一特殊含矿岩性层,含矿层产在大套红褐色泥岩之中,矿层之上发育四层透镜状砂体,砂体规模均不大,发育紫红色和灰绿色两种砂岩,钙质胶结现象明显,均具有铀偏高现象,灰绿色砂岩铀异常值更大。灰绿色泥灰岩矿化层呈透镜状,出露长度7 m,厚度0.35~0.55 m,沿倾向有

延伸的趋势;矿化层分布大量不规则状的硅质团块,矿化与之相关,硅质团块为沉积产出特点,没有穿层和脉体充填现象;矿化层及周围岩层较为完整,少量槽探工程揭露,未发现构造裂缝及其他脉体;矿化层

岩性及颜色较为均一,没有明显后生蚀变改造现象;总体来看,矿化层控现象明显(图4),具有原生沉积的特征。



图4 铀矿化层产出的岩性剖面特征

Fig. 4 Lithologic profile characteristics of uranium mineralization layer

a—铀矿化层剖面照片;b—铀矿化层产出地质剖面图

a—photograph of the uranium mineralization layer profile;b—uranium mineralization layer output geological profile

3 矿化岩性结构及矿物组合

3.1 岩性结构

含矿层最典型的是具有硅质团块状岩性结构,矿化岩性中含分布不匀、数量不等的硅质团块,硅质团块形态大小各异,以不规则团块状、长条状、豆状和米粒状为主(图5a、5b、5c),团块粒径大小在0.5~5 cm之间;铀异常矿化与硅质团块形态大小和数量呈正相关,矿化岩性中硅质团块粒径越大、含量越高则铀含量越高,反之越低(图5)。

矿化层由灰绿色泥灰岩基质主体和黑红色硅质团块两部分构成,两者边界明显,形态不规则(图6a、

6b、6c)。泥灰岩基质部分的结构和成分较为简单,主要为泥晶碳酸盐组成,混杂有少量黏土和粉砂级陆源碎屑(图6d)。黑红色硅质团块的结构和成分较为复杂,大致可以分为基质、斑块和细脉三部分(图6e);基质部分由晶形较差的微晶石英组成;斑块由赤铁矿环边和晶形较好的微晶石英构成,斑块形态不规则,大小不一($100\sim2000\mu\text{m}$);细脉主要是碳酸盐矿物,宽度一般小于 $40\mu\text{m}$,碳酸盐细脉具有切穿微晶石英斑块和硅质团块的现象(图6f),应该是相对晚期的产物。

3.2 矿物组合及铀矿物赋存形态

含矿层泥灰岩基质和硅质团块中的矿物组合有所不同,泥灰岩基质呈现化学沉积和陆源碎屑混积



图5 矿化层硅质团块特征

Fig. 5 Characteristics of siliceous mass in the mineralized layer

a—黑红色硅质团块,以2~5 cm较大粒径团块为主,团块在含矿岩性中含量较高,以交织形状不规则团块为主,伽马能谱测量铀含量为 135×10^{-6} ; b—黑红色硅质团块,以0.5~2 cm中等粒径团块为主,团块含量中等,以较孤立豆状或长条状为主,伽马能谱测量铀含量为 105×10^{-6} ; c—黑红色硅质团块,以小于1 cm粒径较小团块为主,团块含量较低,以孤立米粒状为主,伽马能谱测量铀含量为 67×10^{-6}

a—the black-red siliceous mass is mainly composed of 2~5 cm larger particle size mass, and the mass content is higher in the ore-bearing lithology. It is mainly composed of irregular mass with interwoven shape. The uranium content measured by gamma energy spectrum is 135×10^{-6} ; b—the black-red siliceous agglomerates are mainly 0.5~2 cm medium-sized agglomerates. The content of the agglomerates is medium, mainly isolated bean-like or long strip-like. The uranium content measured by gamma spectroscopy is 105×10^{-6} ; c—the black-red siliceous agglomerates are mainly small agglomerates with a particle size of less than 1 cm. The content of the agglomerates is low, mainly in the form of isolated rice grains. The uranium content measured by gamma energy spectrum is 67×10^{-6}

的矿物组合特征,硅质团块表现为低温热液矿物组合特征,铀矿物仅发育在硅质团块中(图7a)。

泥灰岩矿物组合特征:整体表现为泥晶碳酸盐和黏土矿物混积的特征,常见陆源碎屑石英(图7b)、长石和少量碎屑锆石(7c),并混有不定数量较差晶形的萤石,萤石含量向硅质团块方向逐渐增多,偶见黄铜矿等金属矿物。

硅质团块基质矿物组合及铀矿赋存形式:以微晶石英为主要矿物,常见铀石、萤石和方解石。矿物组合表现为两种形式,一种以微晶石英为主,含有较多的萤石、铀石和碳酸盐矿物,星散状不均匀分布于微晶石英中,还零星分布少量的自然砷、黄铜矿和重晶石;铀矿物赋存状态主要有5种形式:①铀石呈细小的独立矿物浸染状分布于微晶石英中(图7d),这是主要的铀赋存形式;②铀石矿物呈环带状分布于微晶石英中(图7e);③铀石矿物沿萤石边缘及解理缝充填(图7f);④铀石矿物赋存于黄铜矿周边,围绕着黄铜矿分布(图7g);⑤铀石赋存于自然砷矿物中,呈交织状(图7h),表现为交代自然砷的特征,周边还见大量铀石呈浸染状分布于微晶石英中,自然砷与铀矿物的共生现象比较特殊,为首次发现。硅质团块基质还有另一种矿物组合特征,微晶石英、萤石和泥晶碳酸盐混杂在一起,以碳酸盐矿物为主(图7d),不发育赤铁矿红化现象,未见铀石、

黄铜矿、重晶石及自然砷等矿物,不是铀矿物产出形成的矿物组合环境。

硅质团块斑块矿物组合及铀矿赋存形式:斑块由环边和中心两个部分组成,环边主要矿物为铁氧化物,中心部分由晶形较好的微-细晶石英组成,局部可见晶形较好的方解石或萤石矿物与其共生。大部分情况下铀矿物在斑块结构中并不产出,但局部可见环边铁氧化物和中心区域同时出现铀矿物,铀石沿赤铁矿环边分布,呈现铁氧化物与铀石交织现象(图7i),为铀石交代铁氧化物特征;在斑块中心部分铀石呈零星状浸染其中。

硅质团块细脉矿物组合:细脉主要为碳酸盐脉,成分主要是方解石,细脉中较常见萤石(图7d),显示为碳酸盐+萤石的后期流体充填特征。尚未在细脉中发现铀矿物的产出。

4 铀矿化成因分析及意义

4.1 铀矿化成因分析

4.1.1 与传统沉积型(砂岩型)铀矿有较大差异

本文阐述的铀矿化与传统广义砂岩型铀矿均有所区别,应属于特殊的铀矿化成因新类型。

(1) 赋矿岩性特殊。陆相沉积型铀矿(广义砂岩型铀矿)赋矿岩性一般以陆源碎屑物质为主,比如

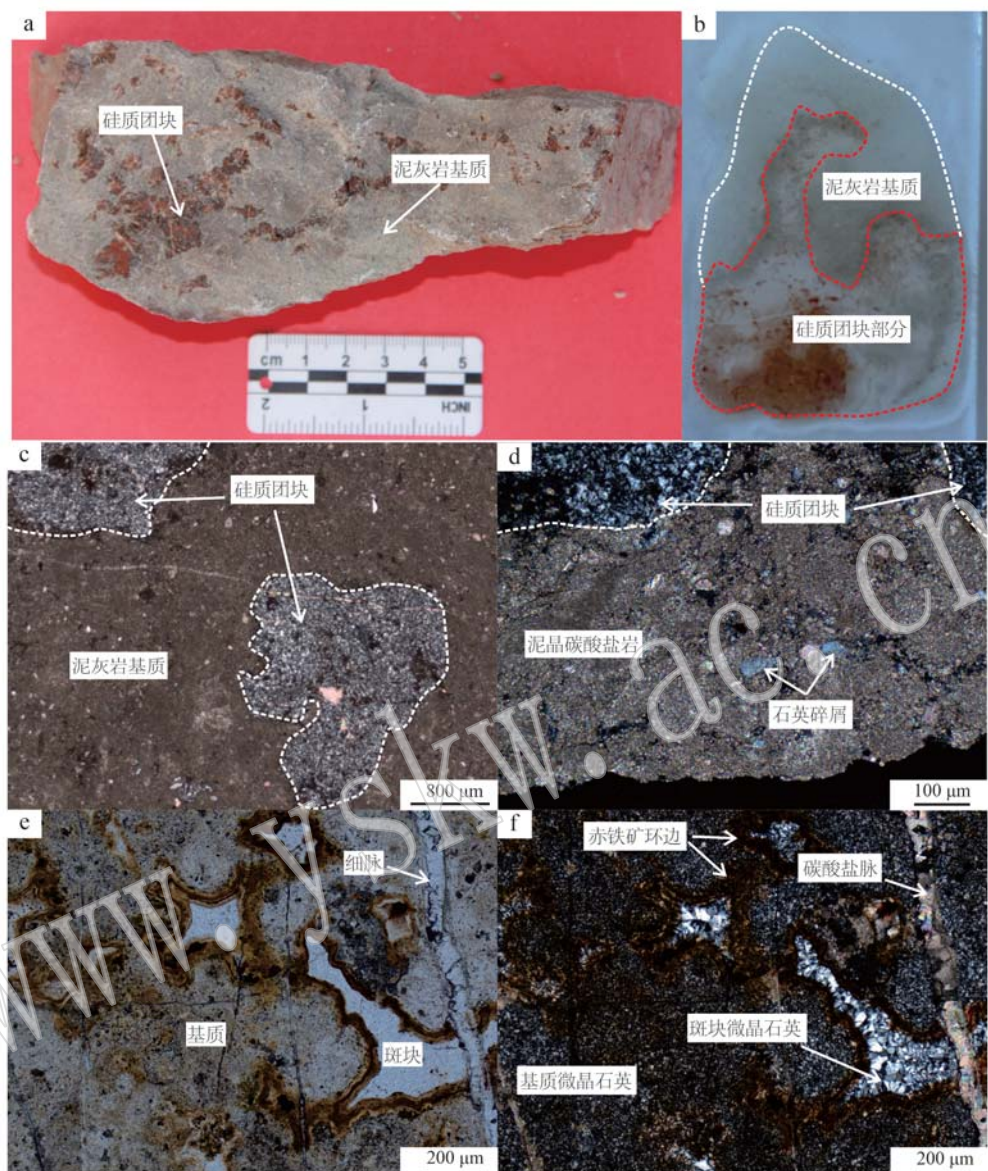


图 6 矿化层岩性结构特征

Fig. 6 Lithological and structural characteristics of mineralized layers

a—灰绿色泥灰岩与黑红色硅质团块构成含矿岩石(手标本); b—泥灰岩基质与硅质团块界线分明(光薄片); c—硅质团块漂浮于泥灰岩基质中(正交偏光); d—泥灰岩基质主要由泥-微晶碳酸盐和少量粉砂级石英碎屑组成(正交偏光); e—硅质团块由基质、斑块和细脉三部分构成(单偏光); f—硅质团块基质由晶形较差的微晶石英组成, 斑块由赤铁矿环边和晶形较好的微晶石英组成, 细脉主要由碳酸盐组成(正交偏光)

a—gray-green marl and black-red siliceous mass constitute ore-bearing rock (hand specimen); b—the boundary between marl matrix and siliceous mass is distinct (polished thin sections); c—the siliceous mass floats in the marl matrix (cross-polarized light); d—the marl matrix is mainly composed of mud-microcrystalline carbonate and a small amount of silty quartz debris (cross-polarized light); e—the siliceous mass is composed of three parts: matrix, plaque and veinlet (plane-polarized light); f—the matrix of siliceous agglomerate is composed of microcrystalline quartz with poor crystal shape, the plaque is composed of hematite rim and microcrystalline quartz with good crystal shape, and the veinlet is mainly composed of carbonate (cross-polarized light)

砾岩、砂岩、泥岩及煤层(张金带等, 2015; 张金带, 2016)。研究的矿化岩性以含硅质团块的灰绿色泥

灰岩为主, 陆源碎屑物质含量较少, 表现为化学沉积岩性特征, 这在陆相沉积盆地比较少见。

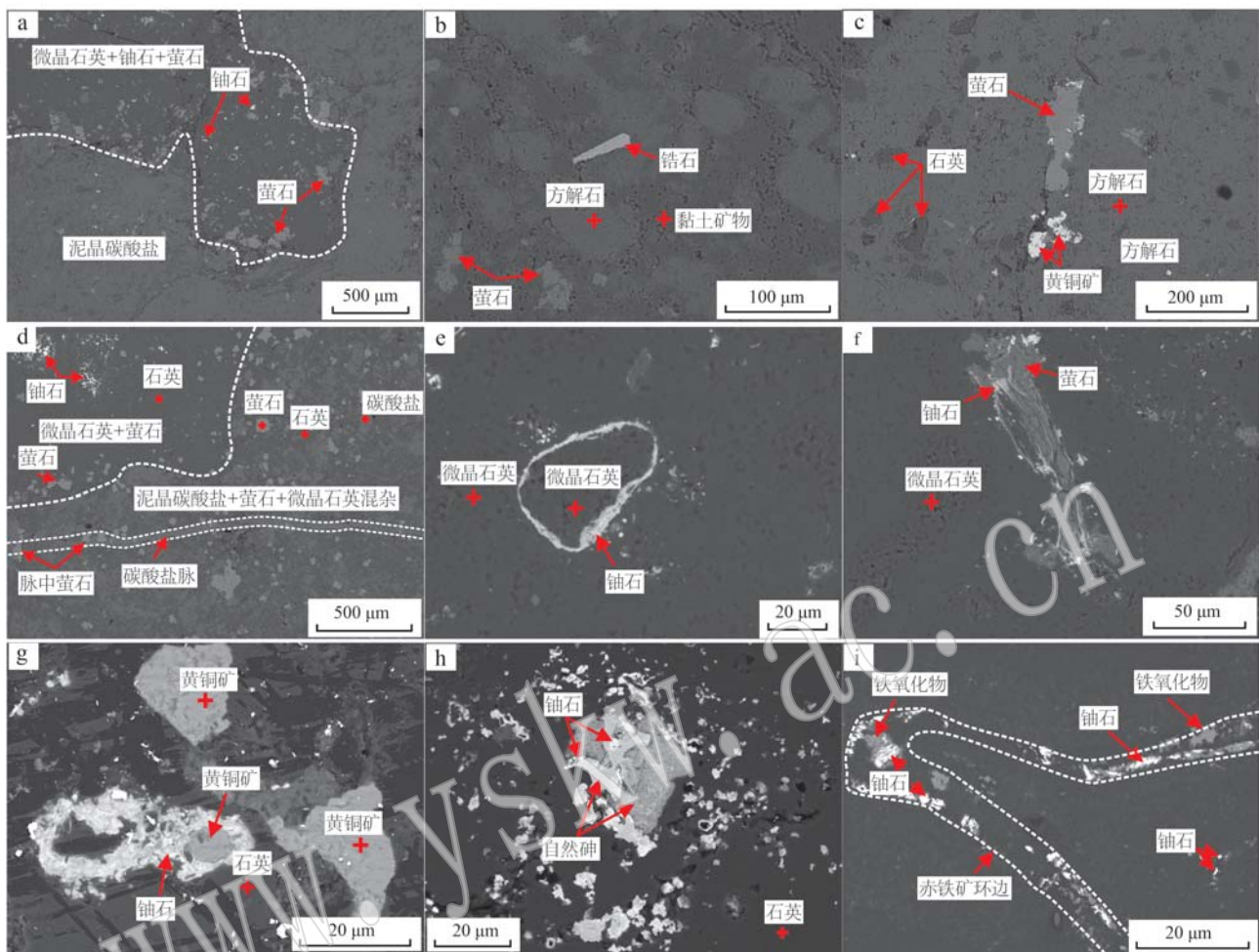


图 7 矿化层铀矿物及矿物组合特征背散射照片

Fig. 7 Backscattered photos of uranium minerals and mineral assemblages in mineralized layers

a—微晶石英中星散状分布的铀石和萤石(硅质团块); b—泥晶方解石、黏土矿物、少量萤石和碎屑锆石混杂堆积(泥灰岩基质); c—泥晶方解石和粉砂级碎屑石英混杂堆积,含少量萤石和黄铜矿(泥灰岩基质); d—微晶石英、铀石和萤石组合(硅质团块的含铀基质),泥晶方解石、萤石和微晶石英组合(硅质团块不含铀基质),方解石和萤石组合(细脉); e—铀石矿物呈环带状分布在微晶石英中; f—铀石沿不规则状萤石的边部及表面分布; g—铀石呈环带状包裹半自形-他形黄铜矿; h—铀石交代半自形自然砷; i—铀石分布在赤铁矿环边和微-细晶石英中心(硅质团块中的斑块)

a—coffinite and fluorite scattered in microcrystalline quartz (siliceous mass); b—mud crystal calcite, clay minerals, a small amount of fluorite and detrital zircon mixed accumulation (marl matrix); c—mud crystal calcite and silt-grade detrital quartz mixed accumulation, containing a small amount of fluorite and chalcopyrite (marl matrix); d—microcrystalline quartz, coffinite and fluorite assemblages (uranium-bearing matrix of siliceous mass), mud crystal calcite, fluorite and microcrystalline quartz assemblages (uranium-free matrix of siliceous mass), calcite and fluorite assemblages (veinlet); e—coffinite are zonally distributed in microcrystalline quartz; f—coffinite is distributed along the edge and surface of irregular fluorite; g—semi-automorphic-anhedral chalcopyrite is wrapped by coffinite; h—coffinite metasomatism semi-automorphic natural arsenic; i—coffinite is distributed in the rim of hematite and the center of micro- microlith quartz (plaques in siliceous mass)

(2) 不具备传统后生改造砂岩型铀矿的条件。缺乏铀富集的物质基础: 传统“水成”铀矿强调铀元素来源沉积盆地富铀蚀源区, 受古环境、古气候、物源搬运及生物作用影响促进铀富集的成矿作用, 尤其是有机质、黄铁矿等还原物质吸附是铀富集成矿的宿主和载体(李洪军等, 2010; 焦养泉等, 2022)。

本次研究的铀矿化层, 是干旱背景下的红杂色岩系, 整体处于氧化环境下, 岩性及镜下观察也未发现有机质和黄铁矿矿物, 只有少量黄铜矿, 矿化层本身是缺乏沉积铀预富集的吸附物质; 富铀碎屑沉积物在一定条件下也可以形成同沉积型铀矿, 但该矿化岩性以细粒泥灰岩为主, 几乎没有富铀碎屑沉积物。

不具备后生改造的特征和条件：传统“水成”铀矿是含铀含氧水沿规模大、连通性和透水性较好的砂岩层运移，并在氧化还原过渡带聚集成矿的过程。本次研究的铀矿化产于湖相沉积环境中，与大型骨架砂体缺乏连通，矿化岩性致密、透水性差，地表含铀含氧水流体难以对其进行成矿改造。热液流体改造也可以使沉积地层中铀发生富集，本文阐述的铀矿化层产出较为完整，层控特征明显，矿化层产状与周围岩层整体产状一致，矿体形态受岩层控制，沿走向和倾向分布，未发现构造裂缝或脉体，后期热液流体改造作用特征不明显。综合产铀层沉积环境、矿体特征及后生改造条件分析，认为铀矿化层属于同生沉积阶段产物。

4.1.2 铀矿化主因——硅质团块成因分析

本文铀矿化与硅质团块密切相关，硅质团块成因分析有助于解释铀矿化成因。关于结核状、团块状硅岩成因解释有多种认识(Bissell, 1959; 刘红光等, 2017; 翟立国, 2020; 郭佩等, 2022)，大多学者认为灰岩中硅质团块为硅质交代碳酸盐岩(Flügel, 2004; 杨锐, 2014)，可能为早成岩阶段产物，也有观点认为硅质团块属于硅质凝胶体或硅质生物壳体直接沉积形成。通过岩石学和镜下观察，研究区硅质团块没有发现古生物特征，可以排除生物成因的可能；从硅质团块产出形态来看，硅质团块具有同沉积-局部交代成因特征：① 硅质团块产于泥灰岩中，这与目前研究发现结核状、团块状常产出于碳酸盐岩之中特征一致；② 硅质团块整体沿顺层分布，局部沿切层方向呈网络状；③ 镜下观察发现硅质团块与泥晶碳酸围岩常呈不规则港湾状；④ 硅质团块中残留部分泥晶碳酸盐，可能为交代后的残余部分。

共生矿物组合是成因判断的重要依据。通过显微镜和扫描电镜及能谱观察，硅质团块共生矿物由红化微晶石英、萤石、铀石、方解石以及少量自然砷、黄铜矿、重晶石构成，显然这样的矿物组合在正常沉积和生物作用下难以形成，尤其是以红化微晶石英、紫黑色萤石和铀矿共生矿物为主的特征，与我国华南地区棉花坑花岗岩硅质脉型铀矿化极其相似(吴德海等, 2019; 李丽荣等, 2021)，显示为中低温酸性热液流体蚀变；铀矿物主要赋存形态也一致，铀矿物浸染状分布于微晶石英中，微晶石英和铀矿物可能为同时沉淀的(刘文泉等, 2022)；不同的是黄铁矿在研究区的硅质团块中不发育，这可能与红色微晶石英形成过程中黄铁矿氧化为铁氧化物所致，并

显示为浅源大气降水与深部流体混合成因。自然砷矿物的发现也十分特殊，因为自然界中自然砷是一种比较罕见的矿物，仅在卡林型金矿和含钨石英脉有所发现(曹东彝, 1986; 谭运金, 2001; 刘家军等, 2007; 安芳等, 2009)，并将其作为卡林型金矿床的标型矿物之一，自然砷的出现往往代表内生作用晚期低温热液在还原环境形成的产物。

通过铀矿化层产出特点、岩性结构、硅质团块矿物组合特征及铀赋存形式综合分析，认为铀矿化硅质团块成因物质可能来源深部酸性热卤水流体，在铀成矿过程中可能存在深循环大气降水加入，研究表明(张祖还等, 1984)铀在F⁻浓度较高的中低温酸性热液，易形成多种氟合铀酰络离子，并以这种形式在酸性介质中迁移，当pH值升高(>6)，这些络离子解体，其中氟与围岩内的钙反应形成CaF₂，铀与萤石一起共沉淀，这与硅质团块中出现大量萤石与铀石共生特点非常一致；再结合硅质团块产出的沉积环境及产状判断，携铀富硅深部低温热液流体于吉迪克组沉积期就进入湖水环境中发生矿化硅质凝胶体沉积，在早成岩阶段发生了交代同沉积的碳酸盐围岩，形成了现在具有同沉积-成岩特征的热液铀矿化硅质团块。

这类与深部热液有关的同沉积型铀矿化类型，在我国北方中新生代陆相沉积型铀矿(广义砂岩型铀矿)中极其罕见和特殊，可以将其归为新的热水沉积成因型。

4.2 成因意义

近年来，关于铀元素是否可以由沉积盆地深部流体直接提供参与砂岩铀成矿作用，成为学者们关注的热点及焦点，深部热液参与砂岩铀成矿的观点也层出不穷(刘章月等, 2016; 聂逢君等, 2021; 刘旭等, 2023; 严兆彬等, 2023; 张成勇等, 2023; 丁波等, 2024)，部分学者提出“渗出铀成矿理论”，认为油气、有机酸及热卤水可将铀进行萃取运移至砂岩中成矿(李子颖等, 2022)；由于砂岩成岩演化过程属于开放体系，成矿作用的直接证据不易发现，大多数从间接蚀变特征及地球化学特征来进行观点说明，争议往往较大，所以很难打破表生铀成矿作用观点束缚。本文的研究直接说明了深部热液及铀元素也是可以进入中新生代沉积盆地甚至陆相红层中发生铀成矿作用，这一观点可带来盆地铀矿找矿新思路。

5 结论

(1) 在前人研究基础上,在塔里木盆地库车坳陷新近纪红杂色层中发现了产于湖相的特殊铀矿化岩性类型,赋矿岩性以化学沉积的灰绿色泥灰岩为主,发育大量不规则的硅质团块,铀矿化强度与硅质团块大小、含量呈正相关,这与传统沉积型铀矿有所区别。

(2) 铀矿物赋存空间及矿物组合显示出低温热液成因特征,铀矿物以铀石为主,呈浸染状赋存于硅质团块的微晶石英中,并与萤石、赤铁矿、黄铜矿、重晶石和自然砷共生,这与我国华南地区硅质脉型铀矿化较为相似;铀矿化硅质团块产出具有同沉积阶段的特征,应属于特殊的热水沉积成因。

(3) 这种产于我国北方新近纪红杂色层的热水成因铀矿化现象,为深部热液携铀进入沉积地层发生铀成矿作用提供了直接有力的证据,强调了深部铀源的重要性,拓展了我国中新生代沉积盆地沉积型铀矿的找矿思路。

致谢 褒心感谢中国核工业集团有限公司、中国核工业地质局对塔里木砂岩型铀矿研究给予的大力支持。褒心审稿专家在审稿过程中提出的建设性修改意见与核工业216大队在资料方面给予的帮助。

References

- A Zhongming, Li Shengfu, Luo Xinggang, et al. 2007. Regional evaluation report of 1:250 000 uranium resource in Wushi-Luntai Area, Tarim Basin, Xinjiang [R]. Urumqi: Geology Party No. 216 (in Chinese).
- An Fang and Zhu Yongfeng. 2009. Significance of native arsenic in the Baogutu gold deposit, western Junggar, Xinjiang, NW China [J]. Chinese Science Bulletin, 54(10): 1 465~1 470 (in Chinese with English abstract).
- Bissell H J. 1959. Silica in sediments of the Upper Paleozoic of the cordilleran Area [J]. SEPM Special Publications.
- Cai Lanpeng, Li Hezhe, Li Laide, et al. 1985. Uranium regional survey in Tianshan area, Xinjiang [R]. Urumqi: Geologic Party No. 216 (in Chinese with English abstract).
- Cao Dongyi. 1986. The discovery of native arsenic in Dajishan tungsten deposits in southern Jiangxi Province, China [J]. Acta Petrologica et Mineralogica, 5(3): 264~268 (in Chinese with English abstract).
- Ding Bo, Liu Hongxu, Xu Deru, et al. 2024. Uranium metallogenetic effect of hydrothermal fluid transformation in sandstone-type uranium deposits in northern Ordos Basin: Constraints from the study of biotite chloritization process [J]. Earth Science, 49(2): 625~638 (in Chinese with English abstract).
- Fliigel E. 2004. Microfacies of Carbonate Rocks [M]. Berlin Heidelberg: Springer-Verlag.
- Guo Pei, Li Changzhi, Wen Huaguo, et al. 2022. Genesis of continental siliceous rocks and their tectonic-climatic significance [J]. Acta Sedimentologica Sinica, 40(2): 450~464 (in Chinese with English abstract).
- Jiao Yangquan, Wu Liqun, Rong Hui, et al. 2022. Sedimentation, diagenesis and uranium mineralization: Innovative discoveries and cognitive challenges in study of sandstone-type uranium deposits in China [J]. Earth Science, 47(10): 3 580~3 602 (in Chinese with English abstract).
- Li Hongjun and Kuang Wenzhan. 2010. Metallogenesis and metallogenetic model of Nuheting uranium deposit in Erlian Basin [J]. World Nuclear Geoscience, 27(3): 125~129 (in Chinese with English abstract).
- Li Lirong, Wang Zhengqi and Xu Deru. 2021. Mineral assemblage characteristics of the Mianhuakeng uranium deposit in northern Guangdong Province and its significance [J]. Acta Petrologica et Mineralogica, 40(3): 513~524 (in Chinese with English abstract).
- Li Shengfu. 2023. Current situation and feature consideration on the uranium exploration in Xinjiang [J]. Uranium Geology, 39(4): 492~497 (in Chinese with English abstract).
- Li Shiqin, Tang Pengcheng and Rao Gang. 2013. Cenozoic deformation characteristics and controlling factors of Kalayergun structural belt, Kuqa fold and thrust belt, southern Tianshan [J]. Earth Science, 38(4): 859~869 (in Chinese with English abstract).
- Li Weifeng, Gao Zhenzhong, Peng Detang, et al. 1996. Sedimentary features and depositional model of Neogene oxidative, broad and shallow brine lake in Tarim Basin [J]. Journal of Jianghan Petroleum Institute, 18(2): 31~35 (in Chinese with English abstract).
- Li Ziying, Liu Wusheng, Li Weitao, et al. 2022. Exudative metallogenesis of the Hadatu sandstone-type uranium deposit in the Erlian Basin, Inner Mongolia [J]. Geology in China, 49(4): 1 009~1 047 (in Chinese with English abstract).
- Liu Gang, Wang Guorong and A Zhongming. 2010. Relations between the structural evolution in Cenozoic and uranium metallogenesis in the north

- of talimu basin[J]. Xinjiang Geology, 28(1): 95~98 (in Chinese with English abstract).
- Liu Hongguang and Liu Bo. 2017. Several genetic models of nodular chert hosted in Phanerozoic carbonate[J]. Geological Bulletin of China, 36(9): 1 635~1 644 (in Chinese with English abstract).
- Liu Jiajun, Yang Dan, Liu Jianming, et al. 2007. Mineralogical characteristics of native arsenic and tracing the metallogenic physicochemical condition in Carlin-type gold deposits[J]. Earth Science Frontiers, 14(5): 158~166 (in Chinese with English abstract).
- Liu Wenquan, Liu Bin, Qi Jiaming, et al. 2022. Geochemical characteristics of red-silicification and implications for uranium mineralization in Mianhuakeng uranium deposit[J]. Uranium Geology, 38(6): 1 084~1 097 (in Chinese with English abstract).
- Liu Xu, Xia Fei, Zhang Chengyong, et al. 2023. Mineralization characteristics of the purplish red uranium ore in the Tamusu uranium deposit within the Bayan Gobi basin[J]. Acta Mineralogica Sinica, 43(3): 325~336 (in Chinese with English abstract).
- Liu Zhangyue, Qin Mingkuan, Liu Hongxu, et al. 2016. Meso-Cenozoic orogeny in South Tianshan and the resultant superimposed enrichment effect on the Sawafuqi uranium deposit[J]. Acta Geologica Sinica, 90(12): 3 310~3 323 (in Chinese with English abstract).
- Lu Kegai, Wang Guorong and Sun Xiao. 2019. Interlayered oxidation-zone styles in fault-fold belts of the northern Tarim Basin and its controlling to the formation of sandstone-type uranium deposits[J]. Journal of Geomechanics, 25(1): 115~124 (in Chinese with English abstract).
- Nie Fengjun, Yan Zhaobin, Xia Fei, et al. 2021. Two-stage and two-mode uranium mineralization for sandstone-type uranium deposits[J]. Acta Geoscientica Sinica, 42(6): 823~848 (in Chinese with English abstract).
- Song Jinpeng, Tian Panpan, Dai Junjie, et al. 2021. Distribution characteristics of gypsum-salt rock and petroleum geological significance in Kuqa Depression of Tarim Basin[J]. Fault-Block Oil & Gas Field, 28(6): 800~804 (in Chinese with English abstract).
- Shi Wenge, Gong Enpu, Chu Yigong, et al. 2015. Sedimentary system and depositional environment of Copper-Bearing rock series of Neogene in Baicheng County, Xinjiang[J]. Acta Sedimentologica Sinica, 33(6): 1 074~1 086 (in Chinese with English abstract).
- Shi Zhilong. 2023. New century's uranium prospecting practice and major breakthrough in Xinjiang[J]. Uranium Geology, 39(4): 481~491 (in Chinese with English abstract).
- Tan Xiucheng, Wang Zhenyu, Li Ling, et al. 2006. Arrangement and evolution of tertiary sedimentary facies in Kuche foreland basin, Xinjiang[J]. Acta Sedimentologica Sinica, 24(6): 790~797 (in Chinese with English abstract).
- Tan Yunjin. 2001. Native arsenic in the carlin type gold deposits[J]. Mineral Resources and Geology, 15(6): 699~704 (in Chinese with English abstract).
- Tang Liangjie, Wan Guimei, Wang Qinghua, et al. 2008. Tectonic evolution of the western Qulitake tectonic belt in Mesozoic and Cenozoic, Kuqa depression[J]. Journal of Southwest Petroleum University (Science & Technology Edition), 30(2): 167~171 (in Chinese with English abstract).
- Wang Guorong, Jiao Yangquan, Chen Zhengle, et al. 2023. Structural constraints of sandstone-type uranium mineralization in Kuqa depression under Basin-mountain coupling mechanism[J]. Uranium Geology, 39(4): 581~594 (in Chinese with English abstract).
- Wang Ke, Xiao Ancheng, Cao Ting, et al. 2008. Geological structures and petroleum exploration fields of the northern tectonic belt in the Kuqa depression, Tarim basin[J]. Acta Geologica Sinica, 96(2): 368~386 (in Chinese with English abstract).
- Wang Ligang. 2004. Study on Deposition and Reservoirs of Neogene Jidike Formation, Kuche Depression[D]. Chengdu: Southwest Petroleum University (in Chinese with English abstract).
- Wang Xinhua, Wu Lisheng, Wang Jinwei, et al. 2023. Evaluation report of 1:250 000 uranium resources in Baozidong-Ridarik area, Tarim Basin, Xinjiang[R]. Urumqi: Geologic Party No. 216 (in Chinese).
- Wang Yuanyuan, Wang Qiangqiang, Lü Junwei, et al. 2023. Unconformity constraint on the neotectonic movement stage and uranium mineralization in Qulitake area, northern margin of Tarim Basin[J]. Uranium Geology, 39(4): 595~605 (in Chinese with English abstract).
- Wu Dehai, Xia Fei, Pan Jiayong, et al. 2019. Characteristics of hydrothermal alteration and material migration of Mianhuakeng uranium deposit in northern Guangdong Province[J]. Acta Petrologica Sinica, 35(9): 2 745~2 764 (in Chinese with English abstract).
- Wu Liqun, Jiao Yangquan, Wang Guorong, et al. 2022. Response of uranium mineralization in Kuqa depression driven by Basin? Mountain coupling mechanism[J]. Earth Science, 47(9): 3 174~3 191 (in Chinese with English abstract).
- Xu Qiang, Qin Mingkuan, Huang Shaohua, et al. 2019. Sedimentary facies feature of Early-Middle Jurassic and implication for uranium mineralization in the north monocline of western Kuche depression[J]. Uranium Geology, 35(3): 129~136 (in Chinese with English abstract).
- Yan Zhaobin, Zhang Wenwen, Zhang Chengyong, et al. 2023. The influ-

- ence of fluid activity from deep basin on the metallogenetic process of sandstone type uranium deposits [J]. *Acta Geologica Sinica*, 97(12): 4 131~4 149 (in Chinese with English abstract).
- Yang Rui. 2014. Analysing on the Origin of Chert: Two Cases Study of Middle Permian Qixia Formation in Chaohu, Anhui and Lucaogou Formation in Urumchi, Xinjiang [D]. Xi'an: Northwest University (in Chinese with English abstract).
- Zhai Liguo. 2020. Study on Siliceous Rock Deposited by Hydrothermal Jet in Continental Lake Basin—A Case Study of Permian Lucaogou Formation in Santanghu Basin, Xinjiang [D]. Xi'an: Northwest University (in Chinese with English abstract).
- Zhang Chengyong, Nie Fengjun, Zhang Xin, et al. 2023. New discovery and significance of sandstone type uranium deposit prospecting in the Bayingebei Basin [J]. *Acta Geologica Sinica*, 97(2): 467~479 (in Chinese with English abstract).
- Zhang Jindai. 2016. Innovation and development of metallogenetic theory for sandstone type uranium deposit in China [J]. *Uranium Geology*, 32(6): 321~332 (in Chinese with English abstract).
- Zhang Jindai, Li Ziyi, Xu Gaozhong, et al. 2015. Great Progress and Breakthrough in Uranium Exploration in China: Examples of Newly Discovered and Proven Uranium Deposits since the Beginning of the New Century [M]. Beijing: Geological Publishing House, 1~442 (in Chinese).
- Zhang Shiben, Ni Yunan, Gong Fuhua, et al. 2003. Guide for Investigation of Peripheral Strata in Tarim Basin [M]. Beijing: Petroleum Industry Publishing House (in Chinese).
- Zhang Xuan, Lin Xiaobing, Yang Huatong, et al. 2023. Migration laws and lithologic assemblages of beach bar sedimentary microfacies of Jidike Formation in Yaha area of Tabei Uplift [J]. *Petroleum Geology & Oilfield Development in Daqing*, 42(6): 26~33 (in Chinese with English abstract).
- Zhang Zuhuan, Zhao Yiyi, Zhang Bangtong, et al. 1984. *Uranium Geochemistry* [M]. Beijing: Atomic Press, 1~403 (in Chinese).
- Zhuang Honghong, Mao Ziqiang, Zhang Tao, et al. 2015. Analysis on mineralization potentiation of sandstone type uranium in Kuche depression of Tarim Basin [J]. *Journal of Xi'an University of Science and Technology*, 35(3): 356~362 (in Chinese with English abstract).
- 1: 25万铀资源区域评价报告 [R]. 乌鲁木齐: 核工业二一六大队.
- 安芳, 朱永峰. 2009. 新疆西准噶尔包古图金矿中的自然砷及其矿床成因意义 [J]. *科学通报*, 54(10): 1 465~1 470.
- 蔡兰朋, 李合哲, 李来得, 等. 1985. 新疆天山地区铀矿区调普查 [R]. 乌鲁木齐: 核工业部西北地勘局二一六大队.
- 曹东彝. 1986. 赣南大吉山钨矿床中自然砷的发现及其研究 [J]. *岩石矿物学杂志*, 5(3): 264~268, 288.
- 丁波, 刘红旭, 许德如, 等. 2024. 鄂尔多斯盆地北缘砂岩型铀矿热液改造的铀成矿效应: 来自黑云母绿泥石化过程的制约 [J]. *地球科学*, 49(2): 625~638.
- 郭佩, 李长志, 文华国, 等. 2022. 陆相硅质岩成因类型及构造-气候指示意义 [J]. *沉积学报*, 40(2): 450~464.
- 焦养泉, 吴立群, 荣辉, 等. 2022. 沉积、成岩与铀成矿: 中国砂岩型铀矿研究的创新发现与认知挑战 [J]. *地球科学*, 47(10): 3 580~3 602.
- 李洪军, 旷文战. 2010. 二连盆地努和廷铀矿床成矿作用及成矿模式 [J]. *世界核地质科学*, 27(3): 125~129.
- 李丽荣, 王正其, 许德如. 2021. 粤北棉花坑铀矿床矿物共生组合特征及其意义 [J]. *岩石矿物学杂志*, 40(3): 513~524.
- 李盛富. 2023. 新疆铀矿勘查的现状和思考 [J]. *铀矿地质*, 39(4): 492~497.
- 李世琴, 唐鹏程, 饶刚. 2013. 南天山库车褶皱-冲断带喀拉玉尔滚构造带新生代变形特征及其控制因素 [J]. *地球科学*, 38(4): 859~869.
- 李维锋, 高振中, 彭德堂, 等. 1996. 塔里木盆地晚第三纪坳陷型氧化宽浅盐湖沉积特征及模式 [J]. *江汉石油学院学报*, 18(2): 31~35.
- 李子颖, 刘武生, 李伟涛, 等. 2022. 内蒙古二连盆地哈达图砂岩铀矿渗出铀成矿作用 [J]. *中国地质*, 49(4): 1 009~1 047.
- 刘刚, 王国荣, 阿种明. 2010. 塔里木盆地北部新生代构造演化与铀成矿作用 [J]. *新疆地质*, 28(1): 95~98.
- 刘红光, 刘波. 2017. 显生宙碳酸盐岩中燧石结核的几种成因模式 [J]. *地质通报*, 36(9): 1 635~1 644.
- 刘家军, 杨丹, 刘建明, 等. 2007. 卡林型金矿床中自然砷的特征与成矿物理化学条件示踪 [J]. *地学前缘*, 14(5): 158~166.
- 刘文泉, 刘斌, 祁家明, 等. 2022. 棉花坑铀矿床红色硅化蚀变岩地球化学特征及对铀成矿的指示 [J]. *铀矿地质*, 38(6): 1 084~1 097.
- 刘旭, 夏菲, 张成勇, 等. 2023. 巴音戈壁盆地塔木素铀矿床紫色铀矿石矿化特征 [J]. *矿物学报*, 43(3): 325~336.
- 刘章月, 秦明宽, 刘红旭, 等. 2016. 南天山中新生代造山作用与萨瓦甫齐铀矿床叠加富集效应 [J]. *地质学报*, 90(12): 3 310~3 323.

附中文参考文献

阿种明, 李盛富, 罗星刚, 等. 2007. 新疆塔里木盆地乌什-轮台地区

- 鲁克改, 王国荣, 孙 漉. 2019. 塔里木盆地北缘断褶带层间氧化带发育样式及砂岩铀矿找矿潜力[J]. 地质力学学报, 25(1): 115~124.
- 聂逢君, 严兆彬, 夏 菲, 等. 2021. 砂岩型铀矿的“双阶段双模式”成矿作用[J]. 地球学报, 42(6): 823~848.
- 宋金鹏, 田盼盼, 代俊杰等. 2021. 塔里木盆地库车坳陷膏盐岩分布特征及油气地质意义[J]. 断块油气田, 28(6): 800~804.
- 时文革, 巩恩普, 褚亦功, 等. 2015. 新疆拜城新近系含铜岩系沉积体系及沉积环境[J]. 沉积学报, 33(6): 1 074~1 086.
- 师志龙. 2023. 新世纪以来新疆铀矿找矿实践与重大突破[J]. 铀矿地质, 39(4): 481~491.
- 谭秀成, 王振宇, 李 凌, 等. 2006. 库车前陆盆地第三系沉积相配置及演化研究[J]. 沉积学报, 24(6): 790~797.
- 谭运金. 2001. 卡林型金矿床中的自然砷[J]. 矿产与地质, 15(6): 699~704.
- 汤良杰, 万桂梅, 王清华, 等. 2008. 库车西秋里塔格构造带中、新生代构造演化[J]. 西南石油大学学报(自然科学版), 30(2): 167~171.
- 王国荣, 焦养泉, 陈正乐, 等. 2023. 盆山耦合机制下库车坳陷砂岩型铀成矿的构造约束作用[J]. 铀矿地质, 39(4): 581~594.
- 王 河, 肖安成, 曹 婷, 等. 2022. 塔里木盆地库车坳陷北部构造带地质结构与油气勘探领域[J]. 地质学报, 96(2): 368~386.
- 王利刚. 2004. 库车坳陷上第三系吉迪克组沉积储层研究[D]. 成都: 西南石油学院.
- 王新华, 邬力生, 王进伟, 等. 2012. 新疆塔里木盆地包孜东——日达里克地区 1: 25 万铀资源评价报告[R]. 乌鲁木齐: 核工业二一大队.
- 王元元, 王强强, 吕俊维, 等. 2023. 塔里木盆地北缘秋里塔格地区新构造运动及铀成矿作用阶段划分——来自不整合的约束[J]. 铀矿地质, 39(4): 595~605.
- 吴德海, 夏 菲, 潘家永, 等. 2019. 粤北棉花坑铀矿床热液蚀变与物质迁移研究[J]. 岩石学报, 35(9): 2 745~2 764.
- 吴立群, 焦养泉, 王国荣, 等. 2022. 盆山耦合机制驱动下的库车坳陷铀成矿作用响应[J]. 地球科学, 47(9): 3 174~3 191.
- 许 强, 秦明宽, 黄少华, 等. 2019. 库车坳陷西段北部单斜带早中侏罗世沉积相特征及其与铀成矿关系[J]. 铀矿地质, 35(3): 129~136.
- 严兆彬, 张文文, 张成勇, 等. 2023. 盆地深部流体活动对砂岩型铀矿成矿过程的影响[J]. 地质学报, 97(12): 4 131~4 149.
- 杨 锐. 2014. 碳酸盐岩中燧石结核与燧石团块成因分析——以安徽巢湖中二叠统栖霞组及乌鲁木齐中二叠统芦草沟组为例[D]. 西安: 西北大学.
- 翟立国. 2020. 陆相湖盆热液喷流沉积的硅质岩研究——以新疆三塘湖盆地二叠系芦草沟组为例[D]. 西安: 西北大学.
- 张成勇, 聂逢君, 张 鑫, 等. 2023. 巴音戈壁盆地砂岩型铀矿找矿新发现与意义[J]. 地质学报, 97(2): 467~479.
- 张金带. 2016. 我国砂岩型铀矿成矿理论的创新和发展[J]. 铀矿地质, 32(6): 321~332.
- 张金带, 李子颖, 徐高中, 等. 2015. 我国铀矿勘查的重大进展和突破: 进入新世纪以来新发现和探明的铀矿床实例[M]. 北京: 地质出版社, 1~442.
- 张师本, 倪寓南, 龚福华, 等. 2003. 塔里木盆地周缘地层考察指南[M]. 北京: 石油工业出版社.
- 张 萱, 林小兵, 杨华童, 等. 2023. 塔北隆起牙哈地区吉迪克组滩坝沉积微相迁移规律及岩性组合[J]. 大庆石油地质与开发, 42(6): 26~33.
- 张祖还, 赵懿英, 章邦桐, 等. 1984. 铀地球化学[M]. 北京: 原子能出版社, 1~403.
- 庄红红, 毛自强, 张 涛, 等. 2015. 塔里木盆地库车坳陷砂岩型铀矿成矿潜力分析[J]. 西安科技大学学报, 35(3): 356~362.